Shear time dependent viscosity of polystyrene-ethylacrylate based shear thickening fluid

2016 Smart Mater. Struct. 25 045005

(http://iopscience.iop.org/0964-1726/25/4/045005)

IOP Publishing Smart Materials and Structures
Smart Mater. Struct. 25 (2016) 045005 (11pp) doi:10.1088/0964-1726/25/4/045005

Shear time dependent viscosity of polystyrene-ethylacrylate based shear thickening fluid

Qian Chen[1], Shouhu Xuan[1], Wanquan Jiang[2], Saisai Cao[1] and Xinglong Gong[1]

[1] CAS Key Laboratory of Mechanical Behavior and Design of Materials, Department of Modern Mechanics, University of Science and Technology of China (USTC), Hefei 230027, People's Republic of China
[2] Department of Chemistry, USTC, Hefei 230026, People's Republic of China

E-mail: gongxl@ustc.edu.cn

Received 27 November 2015, revised 9 February 2016
Accepted for publication 9 February 2016
Published 14 March 2016

Abstract

In this study, the influence of the shear rate and shear time on the transient viscosity of polystyrene-ethylacrylate based shear thickening fluid (STF) is investigated. If the shear rate is stepwise changed, it is found that both the viscosity and critical shear rate are affected by the shear time. Above the critical shear rate, the viscosity of the STF with larger power law exponent (n) increases faster. However, the viscosity tends to decrease when the shear time is long enough. This phenomenon can be responsible for the reversible structure buildup and the breakdown process. An effective volume fraction (EVF) mechanism is proposed to analyze the shear time dependent viscosity and it is found that viscosity changes in proportion to EVF. To further clarify the structure evolution, a structural kinetic model is studied because the structural kinetic parameter (λ) could describe the variation in the effective volume fraction. The theoretical results of the structural kinetic model agree well with the experimental results. With this model, the change in viscosity and EVF can be speculated from the variation of λ and then the structure evolution can be better illustrated.

Keywords: shear thickening, shear time, viscosity, effective volume fraction, structural kinetic model

(Some figures may appear in colour only in the online journal)

1. Introduction

Shear thickening fluid (STF) is a type of non-Newtonian fluid that widely exists in concentrated colloidal suspensions [1–3]. The viscosity of STFs increases by orders of magnitude when the shear rate exceeds a critical value, then decreases to the initial state soon after the applied shear rate is eased [4–6]. Due to the excellent reversible shear thickening effect, STF has been widely used in applications such as soft armor, dampers, liquid couplings, shock absorption, and ballistic protection [7–10].

Multiple theoretical and experimental methods have been adopted to investigate the mechanical behavior of STF [11–14]. The classic hydrodynamic clusters theory believed that the interaction between particles and the short range hydrodynamic lubrication force induced the formation of hydrodynamic clusters, thus they could bear stress when under shear force [5]. This theory has been supported by rheo-optical experiments, neutron scattering, and Stokesian dynamic simulation [15–17]. In colloidal suspensions, the higher volume fraction leads to larger clusters. The viscosity of STF follows the power law function $\tau = K\dot{\gamma}^n$ and n can distinguish the type of STF. If $n > 2$, it belongs to discontinuous shear thickening (DST), whose viscosity will be extremely high, and it can even change to the solid-like state when under a high shear rate. When $1 < n < 2$, it belongs to

continuous shear thickening (CST) and the viscosity grows gently [18].

The volume fraction of the dispersed phase has exhibited great influence on the viscosity of dense suspensions [19, 20]. The viscosity can be expressed as $\eta_r = f(\phi, Pe_{\dot{\gamma}}, Re_{\dot{\gamma}})$, where η_r is relative viscosity, ϕ is volume fraction, and $Pe_{\dot{\gamma}}$, $Re_{\dot{\gamma}}$ are two-dimensional numbers [21]. $Pe_{\dot{\gamma}}$, $Re_{\dot{\gamma}}$ are both regarded as invariants in a steady shear, thus the viscosity is determined by the volume fraction. For a dilute suspension, the relative viscosity can be determined from the volume fraction: $\eta_r = 1 + 2.5\phi + 5.9\phi^2$ [22]. It is found that the viscosity of silica is a kinetic property determined by the concentration of a Si–O molecular ligand determined by the structure and bonding of the silica network [23]. So viscosity is closely associated with the evolution of structure. Moreover, in the time dependent research of alumina suspensions, it was found that the suspensions exhibited pseudoplastic behavior for small shear rates and dilatant behavior for higher shear rates [24]. Mukherjee *et al* reported that the viscosity of the alumina suspensions increased at each of the applied shear rate [25]. In semi-solid metal alloys, viscosity increased at the beginning and then decreased, accompanied by significant particle size change [26]. Above the critical shear rate, slight changes in shear rate have a large effect on viscosity curves [27]. Moreover, the time dependent viscosity change of hydroxypropylcellulose can be fitted accurately by a single exponent and a time constant [28]. An apparent viscosity function relating to the shear rate within three shear thickening zones (first shear thinning, shear thickening, second shear thinning) has also been reported [29].

Thixotropic behavior, which has been used to illustrate the shear-induced change in viscosity and normal force of polymer solutions [30, 31], used to be studied using the test of stepwise changes in shear rate or shear stress, since the coupled effects of time and shear rate or shear stress could be clearly separated in the stepwise test [32]. In finite shear time, the microstructure would reach a new equilibrium by competition between the processes of tearing apart: stress and flow induced collision [32, 33]. When the time scale is significantly longer than the response times of the instruments, time effects become important [32]. The shear rate–shear stress curve of poly(ethylene glycol) solutions (PEG) with different concentrations emerged as a hysteresis loop. There is a stress decay at a steady shear rate after each upward step changes in shear rate [33]. Clearly, the study of time effects on the rheological properties of STF is important for understanding the shear thickening mechanism. The overall changes in viscosity at a constant shear rate and the time dependent responses of viscosity have not been investigated.

In this work, stepwise change tests in shear rate were conducted to investigate the rheological behavior of STFs. The shear time dependent viscosity was illustrated by the effective volume fraction (EVF) mechanism, which was summarized from the classic clusters theory. Viscosity first increased when the shear rate exceeded the critical value. Then the viscosity tended to decrease when the shear time was long enough. Polystyrene-ethylacrylate (PSt-EA) nanosphere suspensions were investigated and the results indicated that the shear time dependent viscosity also exhibited a close relationship with n of the STF. Above the critical shear rate, the viscosity increased quickly when n was large, while a small n led to a low viscosity increment. Combining these results with the dimensionless analysis of viscosity expression, it was concluded that the EVF mechanism explained the viscosity tendency. Furthermore, a structural kinetic model has been proposed to describe the variation in λ. The EVF has been closely associated with the value of λ. The EVF would be large if the value of λ increased. The experimental and theoretical consistency of the structural kinetic model was satisfactory. Thus, this model could be used to speculate the change in viscosity and EVF.

2. Experimental section

2.1. Preparation of PSt-EA nanospheres

All the chemical reagents including styrene (St), potassium persulfate (KPS), acrylate (AA), ethylacrylate (EA) were analytical purity and purchased from Sinopharm Chemical Reagent Co, Ltd. Styrene was purified with NaOH solutions. KPS was handled using the recrystallization method.

PSt-EA nanospheres were prepared by soap free emulsion polymerization. All polymerizations were carried out in a 500 ml three-necked flask fixed with a mechanical stirrer, a reflux condenser and a nitrogen inlet. St, EA and AA were firstly mixed using a mechanical stirrer for 30 min in distilled water. Then, KPS, which was chosen as initiator, was added to the mixture and mixed for 10 min at room temperature. After that, the flask was heated to 75 °C in a water bath for 6 h. All runs were conducted under nitrogen atmosphere. The emulsion obtained was centrifuged and then the sediment was redispersed in distilled water to be cleaned for 30 min using an ultrasonic cleaner. This procedure was iterated three times. Finally, the PSt-EA nanospheres obtained were dried in a vacuum oven at 40 °C.

2.2. Characterization of PSt-EA nanospheres

The microstructure of the nanospheres was investigated by scanning electron microscopy (SEM, Sirion 200) and transmission electron microscopy (TEM). The SEM and TEM images of PSt-EA nanospheres are given in figure 1. The microscopy of PSt-EA nanospheres indicated that the nanospheres were monodisperse. In addition, this type of nanosphere was regularly arranged and no terrible aggregations were found. The average particle size of PSt-EA was estimated to be around 340 nm.

2.3. Preparation of STF of different concentrations

The STFs were prepared by dispersing PSt-EA nanospheres into ethylene glycol. Both dispersed phase and dispersed medium were mixed in a ball crusher and rubbed for 24 h in order to obtain a uniform distribution of nanospheres within the suspensions. In this research, different concentrations of STFs (55 vol.%, 58 vol.%, 61 vol.% and 64 vol.% for PSt-

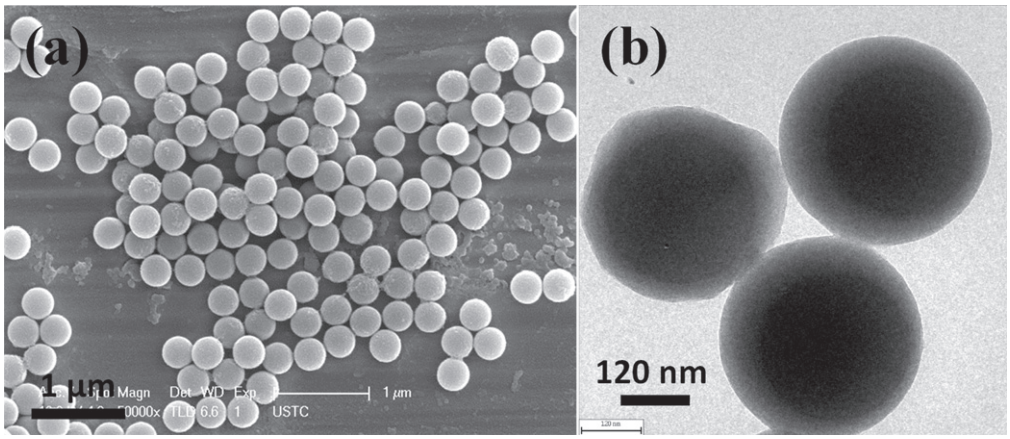

Figure 1. SEM (a) and TEM (b) images of PSt-EA.

Table 1. Power law exponents of all samples.

Sample	Volume fractions	Power law exponents (n)
PSt-EA suspensions-1	55 vol.%	1.90
PSt-EA suspensions-2	58 vol.%	4.89
PSt-EA suspensions-3	61 vol.%	6.89
PSt-EA suspensions-4	64 vol.%	20.90

EA) were obtained by varying the amount of dispersed phase in the dispersed medium.

2.4. Rheological measurements

The experiments were performed primarily in a stress and strain controlled rheometer (Anton-Paar MCR 301) with cone-plate geometry, having a cone angle of 0.2° and a diameter of 25 mm. All the experiments were conducted with a gap size of 0.05 mm at a room temperature of 25 °C. The steady shear test of different measuring times was first - conducted and then the test of how viscosity varies with stepwise changes in shear rate lasting different times was investigated for each sample.

3. Results and discussions

3.1. Steady shear results of PSt-EA suspensions

The shear stress τ and the shear rate $\dot{\gamma}$ of the STF can be fitted by a power law function $\tau = K\dot{\gamma}^n$, and can be further expressed as $\eta = K\dot{\gamma}^{n-1}$. In this function, n is the power law exponent indicating the shear thickening effects, and K is the consistency index. The n of all samples is shown in table 1. Steady shear tests of all samples were conducted using a stress and strain controlled rheometer with cone-plate geometry. By varying the shear time at each measuring point, the intrinsic time dependent viscosity was investigated. In this study, the shear time at each measuring point was set as 10 s, 60 s and 120 s.

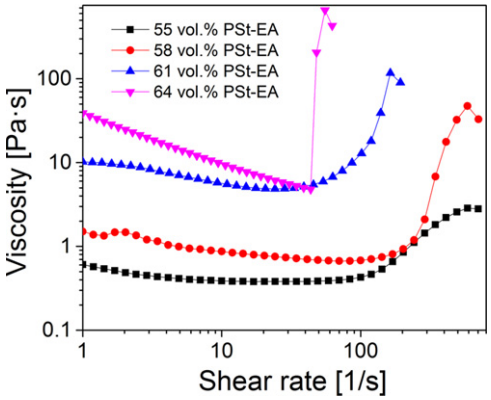

Figure 2. Steady shear tests of PSt-EA suspensions for different volume fractions: 55%, 58%, 61% and 64%.

Figure 2 shows the typical rheological behavior of the STF. With an increase in concentration, the shear thickening effects of the suspensions are strengthened and the viscosity is significantly increased. The shear time represents a critical influence on the maximum viscosity (figure 3). When the power law exponent was small, the viscosity almost kept the same value now matter how the shear time varied (figure 3(a)). With increasing n, the DST behavior of the STF became obvious and then the shear time effect could be found. For 58 vol.% PSt-EA suspensions, the maximum viscosity reached 55 Pa s when the shear time was set to be 10 s, while the maximum viscosities of shear times of 60 s and 120 s were 28 Pa s and 21 Pa s, respectively. Both were much lower than that of the shear time of 10 s (figure 3(b)). At the same shear rate in the shear thickening region, the longer shear time leads to a lower viscosity. Similarly, the other STFs with different concentrations also exhibit this characteristic (figures 3(c) and (d)). It was found that the viscosity increases more sharply with decreasing shear time, and the critical shear rate increases with increasing shear time. Therefore, larger shear time not only delays the onset of shear thickening but also reduces the shear thickening effects.

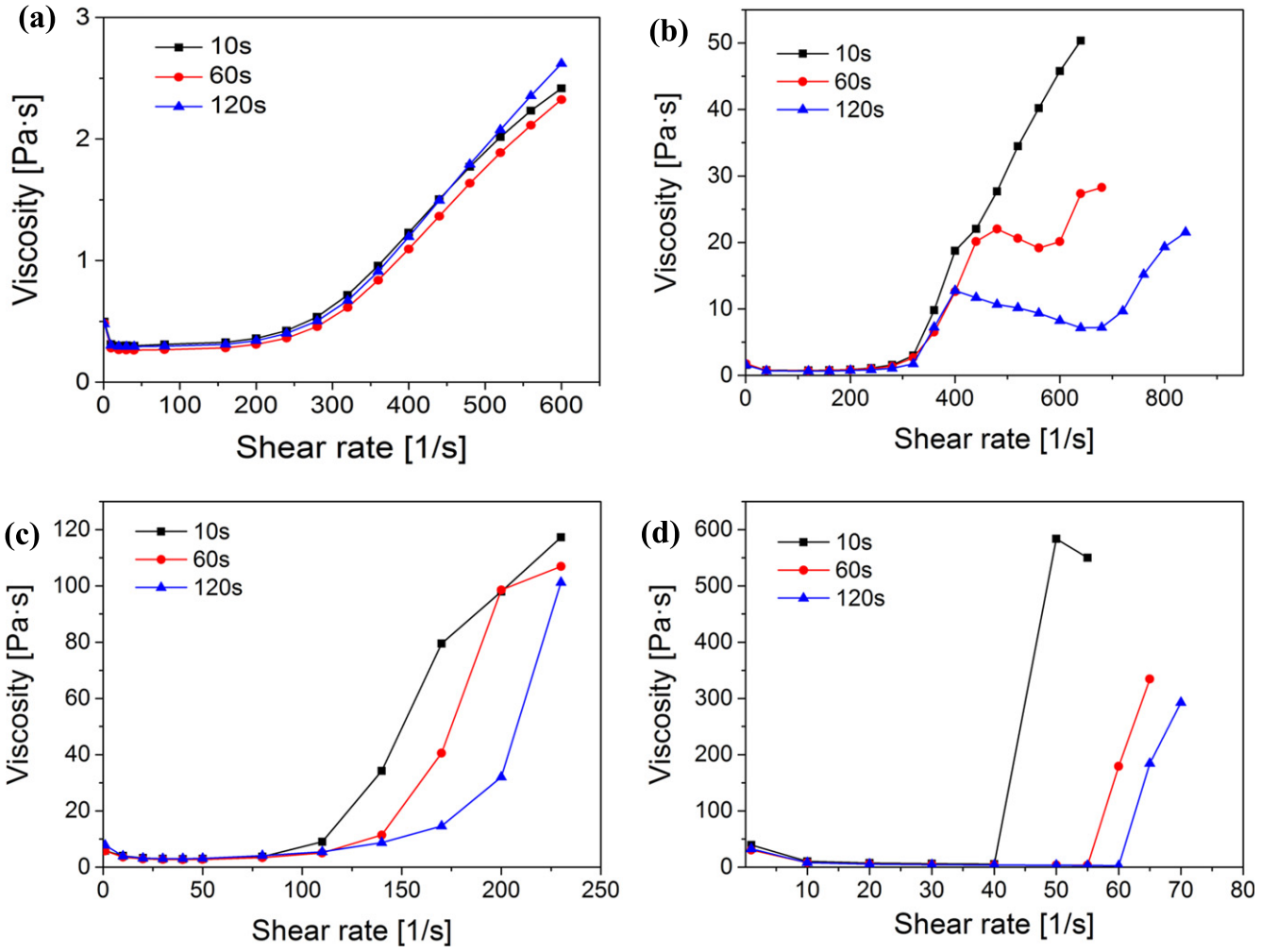

Figure 3. Steady shear tests: viscosity curves at different shear times (10 s, 60 s and 120 s per measuring point). (a) 55 vol.% PSt-EA suspensions, (b) 58 vol.% PSt-EA suspensions, (c) 61 vol.% PSt-EA suspensions, and (d) 64 vol.% PSt-EA suspensions.

3.2. Stepwise change tests in shear rate

To further understand the influence of shear time on shear thickening, stepwise change tests were conducted. For each shear rate, the shear time was set as 10 s, 60 s, and 120 s.

The n for 55 vol.% PSt-EA suspensions was 1.90, and the STF exhibited typical CST behavior (as seen in figure 4(a)). Under different shear times, the characteristics of the time dependent viscosity varied. For simplicity, $\dot{\gamma}_c$ and $\dot{\gamma}_m$ were defined as the critical shear rate and the shear rate when the viscosity reached the maximum value. From figures 4(b)–(d), we can see that the three viscosity curves were similar. If the shear rate exceeded $\dot{\gamma}_c$, the viscosity would increase under the stepwise change in shear rate. The reason is that stepwise change in shear rate causes the increase in cluster amount. If the constant shear rate is only a little larger than $\dot{\gamma}_c$, the viscosity is nearly constant under shear for a period of time. With an increase in shear rate, an obvious decrease in viscosity would be exhibited after a long shear time. When the shear rate was close to $\dot{\gamma}_m$, the buildup rate of the structure was strengthened. In this case, the decrement phenomenon of the viscosity disappeared and the viscosity tended to be a constant. Due to the relatively low shear thickening effects, the scale and number of clusters was not so large and the evolution of the structure was not apparent, thus the viscosity showed less dependency with shear time.

The n for 58 vol.% PSt-EA suspensions was 4.89 (figure 5(a)), thus it exhibited DST behavior. During the testing, the shear rates were set from 1 to 840 s^{-1} to ensure good recording of the viscosity changes. It was found that the viscosity curves varied with different shear time, which meant that the rheological behavior of the STFs was closely associated with shear time. When the shear rate exceeded $\dot{\gamma}_c$, the viscosity increased when the stepwise increased shear rate was applied. The viscosity also kept increasing when STF was continuously sheared at a constant shear rate. As shown in figure 5(b), the viscosity almost kept increasing during all the shear time in each of the shear rates from $\dot{\gamma}_c$ to $\dot{\gamma}_m$. However, when the shear time increased to 60 s per shear rate (figure 5(c)), the viscosity began to decrease if the shear rate reached 440 s^{-1}. Moreover, the decrement disappeared at a shear rate of 600 s^{-1}, since the shear rate was close to $\dot{\gamma}_m$. As soon as the shear time increased to 120 s (figure 5(d)), the viscosity curve became more unique. When the shear rate reached 400 s^{-1}, the viscosity increased at first and then

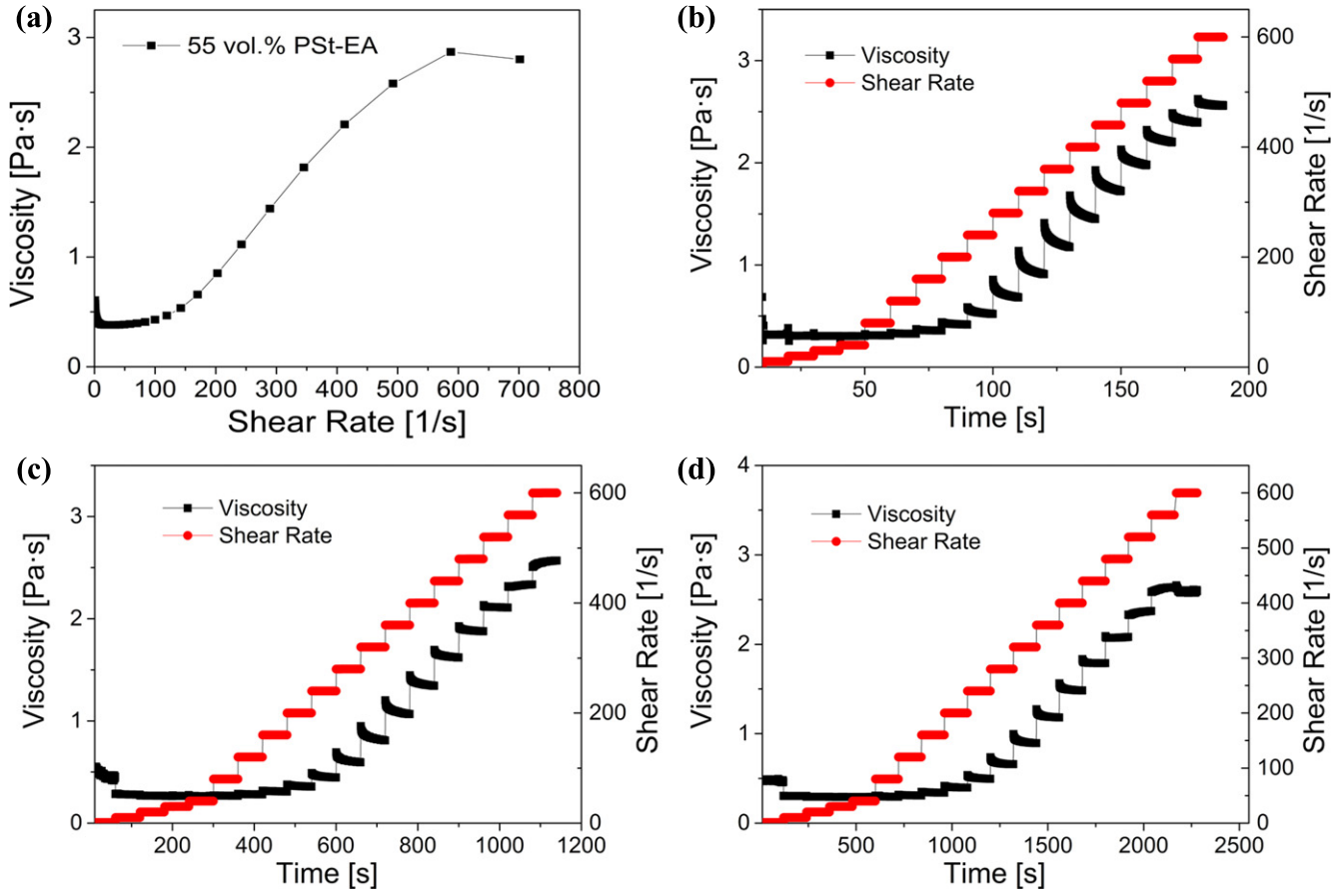

Figure 4. (a) Steady shear results of 55 vol.% PSt-EA suspensions; stepwise change tests in shear rate. Viscosity curves when each shear rate lasted (b) 10 s, (c) 60 s, and (d) 120 s.

decreased with increasing shear time. The same phenomenon could be seen at shear rates from 440 to 720 s^{-1}. When the shear rate was close to $\dot{\gamma}_m$, the viscosity increased again. It should be noted that the viscosity that corresponded to the same shear rate of shear time 10 s was larger than that of the other two conditions, and the viscosity of the shear time 120 s was the smallest.

When the concentration of the PSt-EA increased to 61 vol.%, the n was 6.89 (seen in figure 6(a)). Clearly, the 61 vol.% PSt-EA suspensions presented a stronger shear thickening effect than the 58 vol.% PSt-EA suspensions and its maximum viscosity was larger. During one step shear time, the viscosity increased at the constant shear rate exceeding $\dot{\gamma}_c$ (figure 6), which was much different to the above result. It can be seen that $\dot{\gamma}_c$ of the testing of 10 s, 60 s, and 120 s are 110 s^{-1}, 140 s^{-1}, and 170 s^{-1}, respectively. This result indicates that long shear time increases the $\dot{\gamma}_c$ of the STF and delays the appearance of shear thickening. Finally, when the shear time was 10 s, the viscosity that corresponded to the same shear rate was larger than that when the shear time was 60 s and 120 s.

A strong DST effect was found for 64 vol.% PSt-EA suspensions with n of 20.90 (figure 7). When the shear rate reached $\dot{\gamma}_c$, there was a quick increment in viscosity and the sample changed into a solid-like state. After that, the solid-like state in the cone-plate geometry was damaged by shear and the viscosity decreased. Thus, the measured $\dot{\gamma}_c$ was equal to the measured $\dot{\gamma}_m$. In this case, the viscosity decreased with increasing shear time. The inset of figure 7(d) shows a detailed description of the viscosity curve when the shear time was 120 s. Keeping the shear rate and shear time at 65 s^{-1} and 120 s, it was found that the viscosity kept constant at first and then had a sudden increase. There was a time lag between the change in shear rate and increase in viscosity. This means that the phenomenon of hysteresis can be seen in the viscosity curve. Similar results were obtained when the shear time was 10 s and 60 s. From figures 7(b)–(d), it can be found that $\dot{\gamma}_c$ increased from 50 s^{-1} to 60 s^{-1}, and to 65 s^{-1}, so shear time can also affect the onset of shear thickening.

3.3. Effective volume fraction (EVF)

The viscosity of the suspensions with monodisperse nanospheres can be calculated by a general function $\eta_r = f(\phi, Pe_{\dot{\gamma}}, Re_{\dot{\gamma}})$, where η_r is relative viscosity, ϕ is volume fraction and $Pe_{\dot{\gamma}}$, $Re_{\dot{\gamma}}$ are two-dimensional numbers [21]. For steady shear, $Pe_{\dot{\gamma}}$, $Re_{\dot{\gamma}}$ can be both regarded as invariants when the shear rate is fixed, thus the viscosity is determined by the volume fraction and the changes in viscosity are responsible for the variation in volume fraction. In the stepwise shear rate test, the volume fraction is a constant value. Under the application of the shear rate or shear

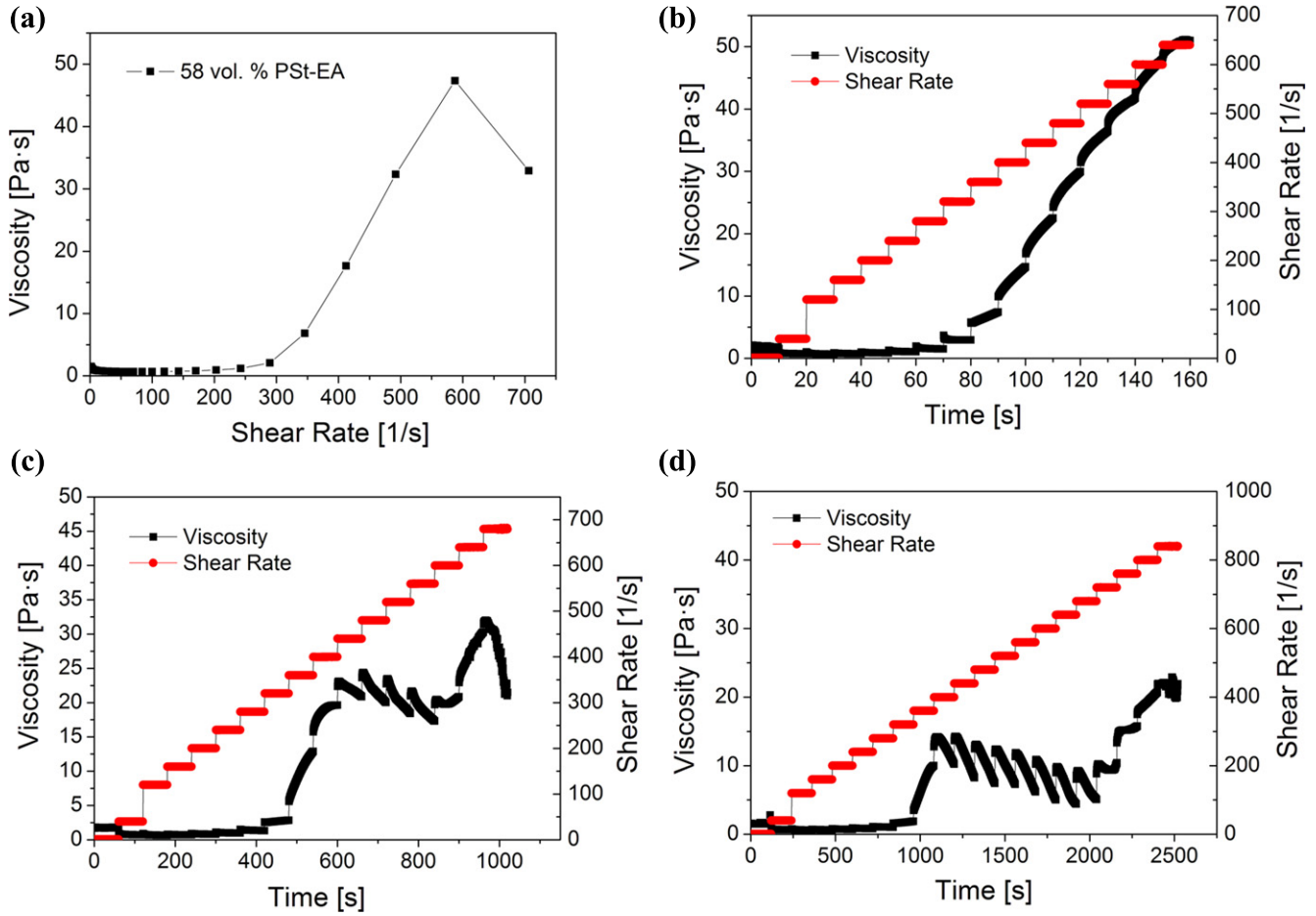

Figure 5. (a) Steady shear results of 58 vol.% PSt-EA suspensions; stepwise change tests in shear rate. Viscosity curves when each shear rate lasted (b) 10 s, (c) 60 s, and (d) 120 s.

stress, the clusters built by nanospheres will change their inner structures. In this case, the disperse medium locked in the center of the clusters, which is described as the 'restrained disperse medium', contributes little to the lubrication and friction in shear thickening (figure 8). Meanwhile, the disperse medium surrounding the nanospheres is regarded as the 'free disperse medium', which is effective for shear thickening. The total volume of nanospheres and restrained disperse medium are the effective volume that affects the shear thickening behavior. The expression of the EVF is as follows:

$$\phi_e = \frac{V_p + V_{rm}}{V} = \frac{V_p + V_{rm}}{V_p + V_{fm} + V_{rm}} \quad (1)$$

where ϕ_e is the EVF, V_p is the volume of nanospheres, V_{rm} is the volume of the restrained disperse medium, and V_{fm} is the volume of the free disperse medium.

In fact, the unique viscosity changes under different shear time are responsible for the variation in the EVF. Without shear, the nanospheres are uniformly distributed in suspensions (figure 8(a)). With an increase in the shear time, these nanospheres tend to aggregate. Then, the as-formed clusters are freely dispersed in the medium and some medium is restrained in the clusters (figures 8(b) and (c)). If the shear time is long enough, the cluster structure will be partly damaged and a layer-like structure will be formed in suspensions. Due to the decrement of the number and scale of clusters, both the EVF and the viscosity of the STF decrease (figure 8(d)). This analysis agrees well with the experimental result. Because of the applied stress and inner friction, the scale of clusters became small after shear for a long time. The volume of the free disperse medium increased and the EVF decreased (as seen in figure 8).

In addition, it is found that the $\dot{\gamma}_c$ decreases with increasing shear time and the viscosity increases more sharply with decreasing shear time in this work. The number of clusters is dependent on the previous structure and shear rate. When suffering a stepwise increased shear rate, the total number of clusters changed. When sheared at a rate lower than $\dot{\gamma}_c$, the structure became more stable with increasing shear time and then the EVF was reduced. Therefore, shear thickening is delayed and $\dot{\gamma}_c$ increases. On the other hand, the more stable structure means a low EVF. As a result, the viscosity is lower at the same shear rate, when shear time is longer.

3.4. Structural kinetics model

Most of the structural kinetics models have been based on a numerical scalar measure to describe the instantaneous level of structure. The numerical scalar is often designated by λ, of

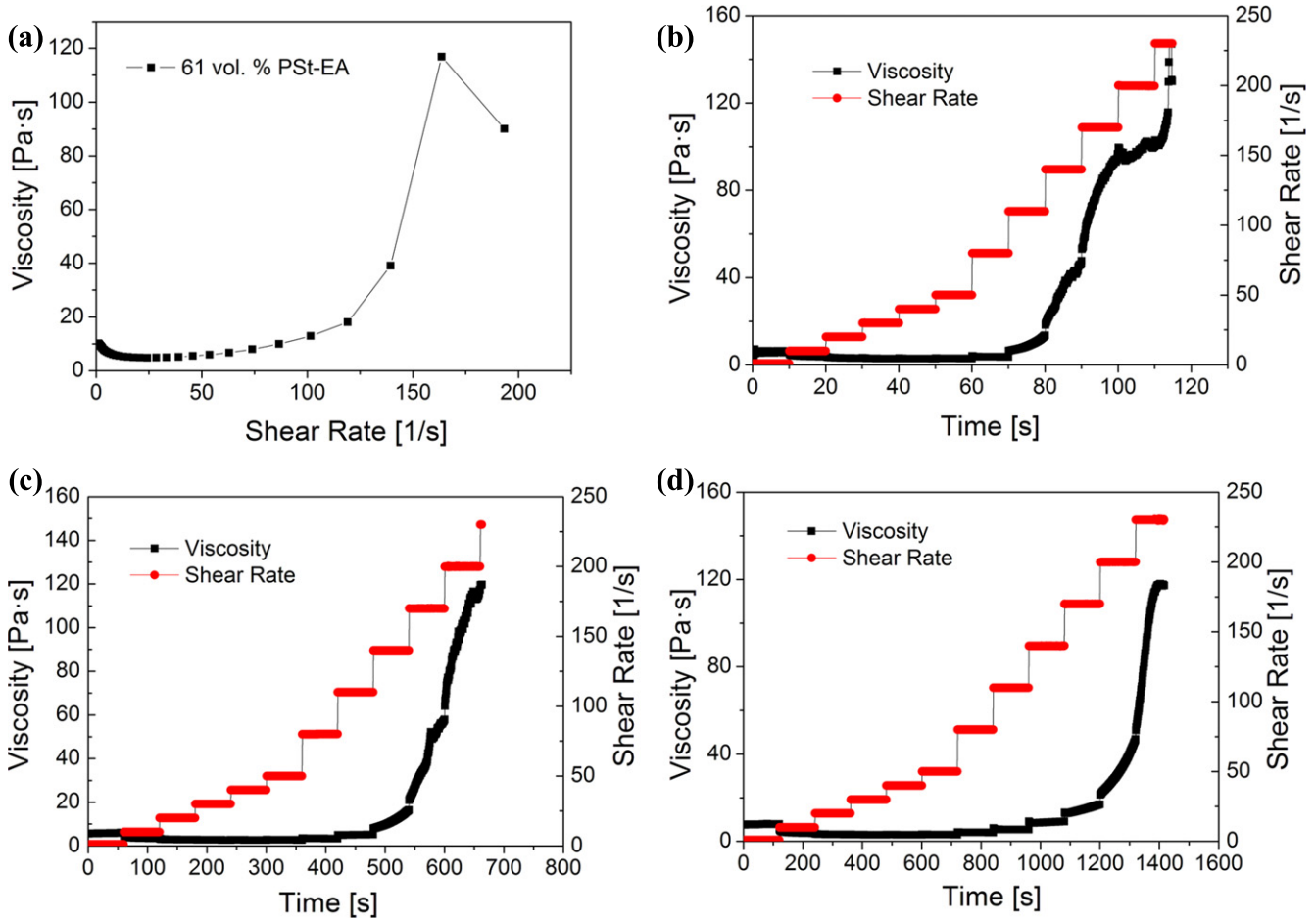

Figure 6. (a) Steady shear results of 61 vol.% PSt-EA suspensions; stepwise change tests in shear rate. Viscosity curves when each shear rate lasted (b) 10 s, (c) 60 s, and (d) 120 s.

which the value varies from 0 to 1. Usually, a completely built structure is represented by $\lambda = 1$ and the completely broken-down structure is represented by $\lambda = 0$ [30, 32]. If λ gets close to 1, the structure tends to be completely built, thus the EVF will rise and then the viscosity will increase. On the other hand, if λ becomes small, the EVF will decrease and so will the viscosity. When sheared at a constant shear rate, the buildup rate of the structure is closely associated with $\frac{\dot{\gamma} - \dot{\gamma}_c}{\dot{\gamma}_m - \dot{\gamma}_c}$. In addition, the previously existing structure, which can be expressed by λ, can also affect the buildup rate. At the same time, the shear stress that accompanied the previously existing structure makes contributions to the broken-down - structure. Thus, the kinetic equation for the structural parameter in this question can be written in the following form:

$$\frac{d\lambda}{dt} = g(\dot{\gamma},\ \lambda,\ n) = \frac{b(1-\lambda)}{t^a}\left(\frac{\dot{\gamma} - \dot{\gamma}_c}{\dot{\gamma}_m - \dot{\gamma}_c}\right)n - c\lambda\dot{\gamma}^d \quad (2)$$

where a, b, c, and d are constants for one system; n is the power law exponent; $\dot{\gamma}$ is the shear rate; $\dot{\gamma}_c$ is the critical shear rate; and $\dot{\gamma}_m$ is the shear rate when the viscosity reaches the maximum value. The first item on the right-hand side of equation (2) represents the buildup rate of the structure and the second item represents the break-down rate. Moreover, in stepwise change tests, shear thickening usually occurred due to an increase in the total number of clusters. Equation (3) provides a general format for a basic constitutive equation of inelastic thixotropy:

$$\sigma(t) = \sigma_y(\lambda) + \eta_\lambda(\lambda)\dot{\gamma} + \eta_{\lambda=0}(\dot{\gamma})\dot{\gamma} \quad (3)$$

where $\eta_{\lambda=0}(\dot{\gamma})$ expresses the residual viscosity when the thixotropic structure is completely broken down. In this work, $\eta_{\lambda=0}(\dot{\gamma})$ can be considered as the viscosity of ethylene glycol. Thus, this term is ignored because the value of the ethylene glycol viscosity is much lower than that of STF. So the expression of viscosity can be written as equation (4):

$$\eta(t) = \frac{\sigma_y(\lambda)}{\dot{\gamma}} + \eta_\lambda(\lambda, \dot{\gamma}). \quad (4)$$

In previous work, various thixotropic models have been put forward [34, 35]. Some relations between rheological parameters, such as $\sigma_{y,0}$ and K_0, and the structure parameter has already been discussed in Houska and other models. Based on their research and reviews [32, 36], we

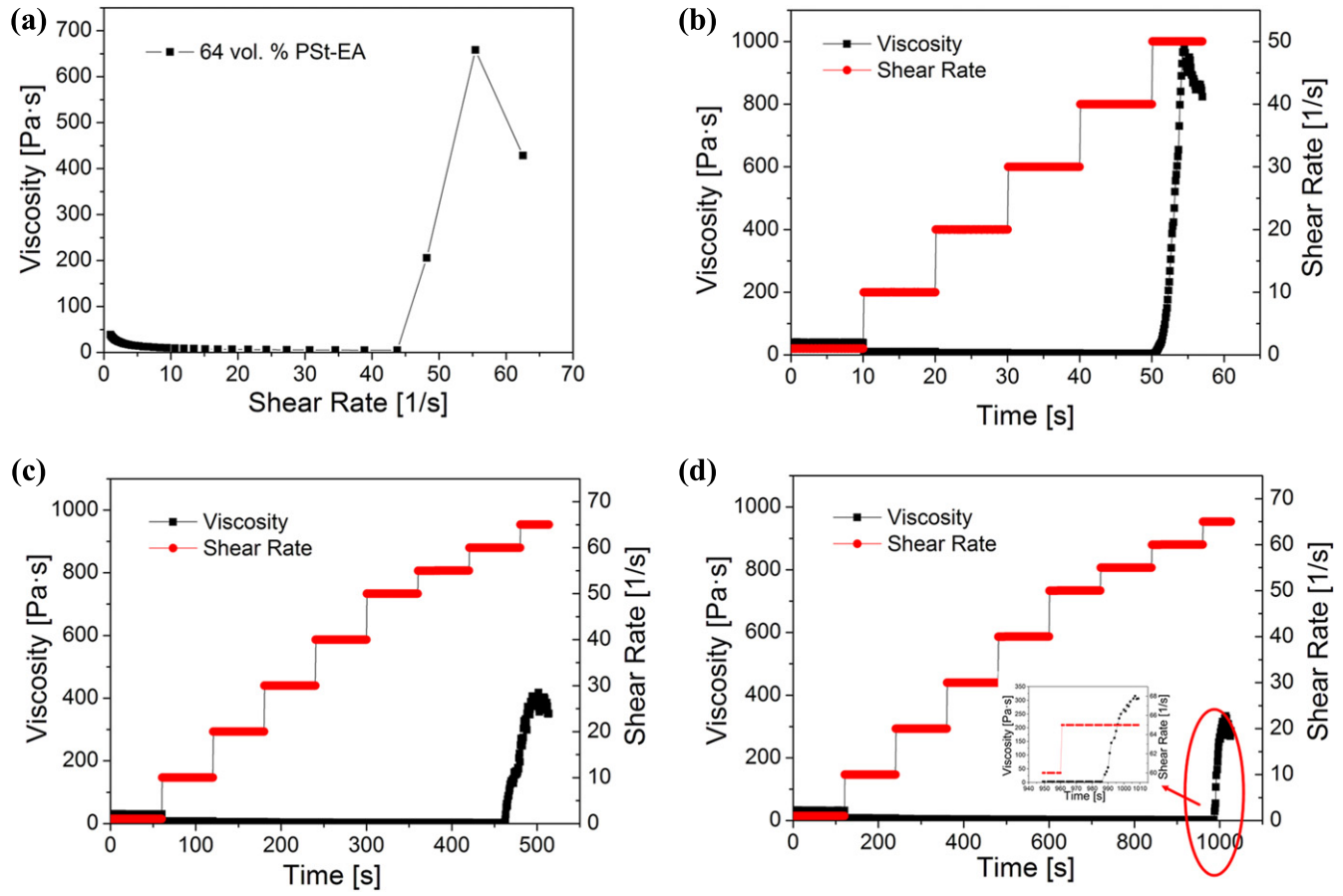

Figure 7. (a) Steady shear results of 64 vol.% PSt-EA suspensions; stepwise change tests in shear rate. Viscosity curves when each shear rate lasted (b) 10 s, (c) 60 s, and (d) viscosity curve when shear time was 120 s and detailed description.

consequently developed the equation of viscosity as follows:

$$\eta(t) = \frac{\lambda\sigma_{y,0}}{\dot{\gamma}} + \lambda K_0 \dot{\gamma}^{n-1}. \quad (5)$$

The model parameters were fitted from the stepwise change test of 58 vol.% PSt-EA suspensions and the shear time was 60 s (figure 9). In fact, the experimental results in the whole shear thickening region can be explained by the proposed model. For a brief expression, viscosity curves at the shear rates of 440 s^{-1}, 480 s^{-1} and 520 s^{-1} were representatively adopted to verify the availability of this model. In the procedure of model parameters fit, the initial and final viscosity of each shear rate were considered as the boundary conditions and the model parameters were adjusted to make the profile of the fit curves approximate to the experimental data. Then the model parameters were used to predict the viscosity curves of the stepwise changes test when the shear time was 10 s and 120 s. In the procedure of prediction, the viscosity when t = 0 s was chosen as the initial condition. In figure 9, it can be seen that the curves of the experimental and theoretical viscosity are almost the same. The experimental and theoretical consistency of the structural kinetic model is satisfactory. Only small differences can be seen in the predictive curve. When the shear time was 10 s, the predicted viscosity was lower than the measured viscosity. When shear time was 120 s, the results were just the opposite. The term $c\lambda\dot{\gamma}^d$ in equation (2) represents the break-down rate of the structure. At a fixed shear rate, $c\dot{\gamma}^d$ was assumed to be a constant for 58 vol.% PSt-EA suspensions. However, the interaction between the as-formed clusters are strengthened with increasing shear time. The real value of $c\dot{\gamma}^d$ of shear time 10 s was smaller than that of shear time 60 s. Meanwhile, the value of $c\dot{\gamma}^d$ of shear time 60 s was used to predict the other viscosity curves. So the predicted viscosity was lower than the measured viscosity when the shear time was 10 s. As seen in figure 9, it is found that the deviation between the measured and predicted viscosity is not apparent so that the structural kinetic model can be used to predict the shear time dependent viscosity.

The evolution of the structure is dependent on the shear rate and it further affects the shear thickening effects. In the structure buildup process, nanospheres begin to move together to form clusters. So the volume of free dispersed medium decreases and the effective volume fraction increases. In the structure break-down process, nanospheres begin to move away from each other and the scale of clusters reduces. So the volume of the free dispersed medium increases and the effective volume fraction decreases. Thus, the structure forming and breaking processes are accompanied by a variation in the EVF. The number of clusters in the STF is in a balance state with the buildup and break-down evolution.

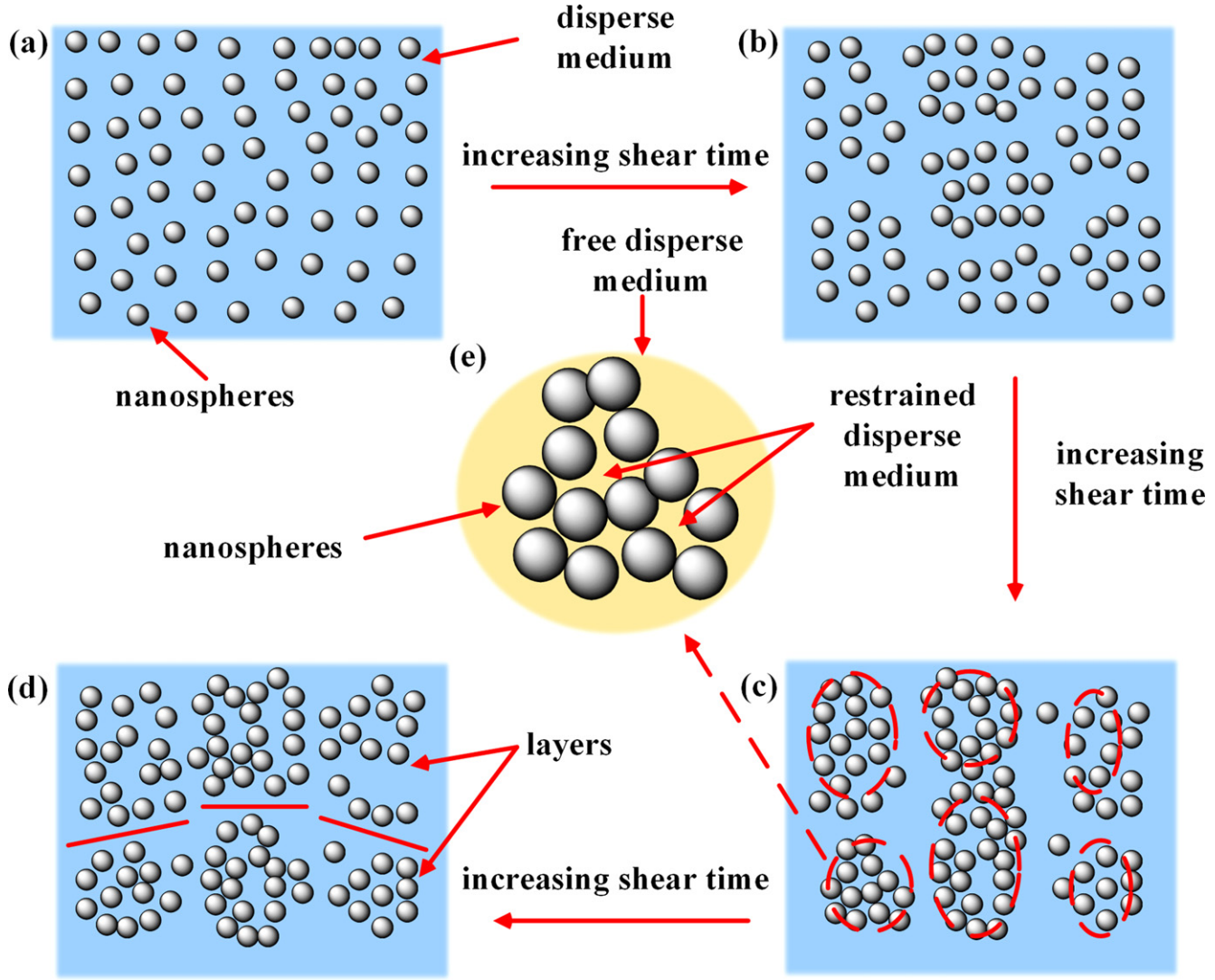

Figure 8. Schematic illustrations of the evolution of structures with increasing shear time: (a) equilibrium, (b) buildup of the structure, (c) formation of clusters, (d) changes in clusters after a long time shearing, (e) free disperse medium and restrained disperse medium.

When the shear rate is lower than $\dot{\gamma}_c$, the viscosity almost stays constant and shear thickening will not take place. If the shear rate exceeds $\dot{\gamma}_c$, the total number of clusters goes up and the structure in the sample will vary. Under constant shear, the shear stress will damage the existing structure. The buildup and break-down rates of the aggregated structure determine the evolution of clusters. When the shear rate exceeds $\dot{\gamma}_c$, the nanospheres will firstly move toward each other to form clusters. The break-down rate of the structure is determined by the current structure and shear rate. With the buildup of the structure, the buildup rate will be restrained and break-down rate will be strengthened. A larger shear rate increases the break-down rate. If the shear time is long - enough, the break-down rate becomes larger than the buildup rate. So the value $\frac{d\lambda}{dt}$ is negative, the structure tends to be damaged and the volume of free dispersed medium increases. This procedure was expressed in the measured curves; viscosity decreased after the increasing stage (figure 5). Thus, the EVF of the STF is changed and the viscosity is influenced. At the same time, the buildup rate of the structure, which is dependent on the shear rate, affects the STF behavior via influencing the current structure. For the STF with a larger n, the buildup rate is higher, thus the rising curves of viscosity are steeper. In addition, the buildup rate of the structure increased when the value of $\dot{\gamma}_c$ became close to $\dot{\gamma}_m$. When the structure is nearly built up completely, the buildup rate reduces and the shear stress breaks down the structure. So viscosity decreased dramatically after reaching the highest value (figure 7). If n is relatively small, the buildup rate will be lower than the break-down rate so the total number of clusters will decrease. Thus, the EVF and viscosity decrease. When the shear rate nearly reaches $\dot{\gamma}_m$, the EVF becomes larger and the viscosity returns to increase.

Table 1 shows the power law exponents of all samples. The experiment results of 55 vol.% PSt-EA suspensions (figure 4) demonstrate that the viscosity firstly decrease and then tends to stay constant with increasing shear rate. With the rise in shear rate, the break-down rate of the structure increases. The buildup rate of the structure cannot increase, apparently because the exponent was not large enough.

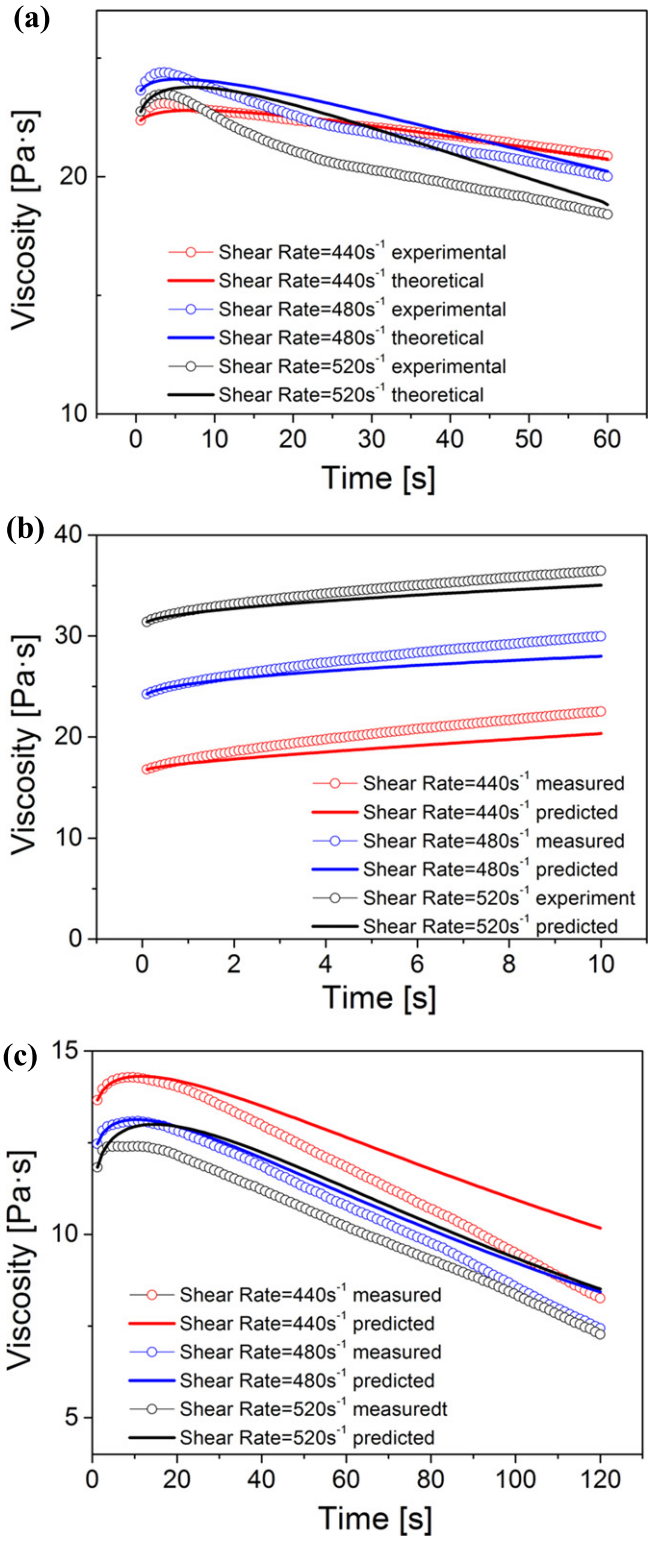

Figure 9. Model predictions of stepwise change tests at different - shear rates (440 s^{-1}, 480 s^{-1} and 520 s^{-1}); (a) experimental and theoretical results when the shear time was 60 s; measured and predicted results when shear time was 10 s (b), and 120 s (c).

Therefore, the EVF will decrease and then an obvious decrease in viscosity would occur. If the n is very large, the buildup rate will be significantly increased and then the EVF will rise, thus the viscosity keeps increasing (such as the results of 61 vol.% PSt-EA and 64 vol.% PSt-EA suspensions shown in figures 6 and 7). The power law exponent is 4.89 for 58 vol.% PSt-EA suspensions (figure 5). The short shear time (10 s) leads the viscosity to keep increasing, while the longer ones (60 s and 120 s) make the viscosity firstly decrease and then increase. The reason is that longer shear time reduces the buildup rate while the break-down rate of the structure stays fairly steady; then the EVF will decrease. As for 61 vol.% PSt-EA and 64 vol.% PSt-EA suspensions, the power law exponents are relatively large and 120 s is not long enough to observe the decrease in the viscosity. The power law exponent for 64 vol.% PSt-EA suspensions is very large and the DST effect occurs. A sudden increase in viscosity is observed when sheared at a constant shear rate rather than the stepwise change in shear rate. When the shear rate is changed from 40 s^{-1} to 50 s^{-1}, the increment of the clusters is not large enough. Because the EVF could not reach the critical value, the phenomenon of shear thickening was not observed. If the shear rate increases to 50 s^{-1}, the buildup rate of the structure is so large that clusters are soon formed and the EVF soon increases to the critical value for shear thickening. Therefore, a steep increase in viscosity is observed. Based on the above analysis, it can be concluded that shear time can affect the behavior of shear thickening.

4. Conclusions

This work studied the shear time dependent viscosity of STFs, in which both the viscosity and critical shear rate were dependent on the shear time. An EVF mechanism is proposed and the shear rate dependent viscosity is analyzed. The relation between the power law exponents and the time dependent viscosity changes can also be explained by a mechanism of the EVF. A kinetic model for the structural parameter is concluded to better illustrate the changes in viscosity and structure. The variation in the EVF is proportional to the kinetic parameter λ. The virtually identical results of the - measured and predicted viscosity curves demonstrated that the structural kinetic model was appropriate for analyzing the shear time dependent viscosity. It was found that increasing the shear time delayed the onset of shear thickening and decreased the value of the viscosity corresponding to the same shear rate. When the power law exponent is low, the - viscosity just decreases under continuous shear at a low rate and then tends to stay constant when the shear rate increases and gets close to $\dot{\gamma}_m$. In a larger power law exponent STF, the viscosity will first increase and then decrease with increasing shear time. When the power law exponent is large enough, the DST effects become very significant and viscosity will keep increasing during all the shear time.

Acknowledgments

This work was supported by Collaborative Innovation Center of Suzhou Nano Science and Technology. Financial supports from the National Natural Science Foundation of China

(Grant Nos. 11372301, 11125210) and the National Basic Research Program of China (973 Program, Grant No. 2012CB937500) are gratefully acknowledged.

References

[1] Barnes H A 1989 Shear-thickening (dilatancy) in suspensions of nonaggregating solid particles dispersed in newtonian liquids *J. Rheol.* **33** 329–66

[2] Hoffman R L 1998 Explanations for the cause of shear thickening in concentrated colloidal suspensions *J. Rheol.* **42** 111–23

[3] Boersma W H, Laven J and Stein H N 1990 Shear thickening (dilatancy) in concentrated dispersions *AlChE J.* **36** 321–32

[4] Laun H M 1991 Rheology of extremely shear thickening polymer dispersionsa) (passively viscosity switching fluids) *J. Rheol.* **35** 999–1034

[5] Wagner N J and Brady J F 2009 Shear thickening in colloidal dispersions *Phys. Today* **62** 27–32

[6] Fall A, Huang N, Bertrand F, Ovarlez G and Bonn D 2008 Shear thickening of cornstarch suspensions as a reentrant jamming transition *Phys. Rev. Lett.* **100** 018301

[7] Gong X L, Xu Y L, Zhu W, Xuan S H, Jiang W Q and Jiang W F 2013 Study of the knife stab and puncture-resistant performance for shear thickening fluid enhanced fabric *J. Compos. Mater.* **48** 641–57

[8] Lee Y S, Wetzel E D and Wagner N J 2003 The ballistic impact characteristics of Kevlar (R) woven fabrics impregnated with a colloidal shear thickening fluid *J. Mater. Sci.* **38** 2825–33

[9] Zhang X Z, Li W H and Gong X L 2008 The rheology of shear thickening fluid (STF) and the dynamic performance of an STF-filled damper *Smart Mater. Struct.* **17** 035027

[10] Decker M J, Halbach C J, Nam C H, Wagner N J and Wetzel E D 2007 Stab resistance of shear thickening fluid (STF)-treated fabrics *Compos. Sci. Technol.* **67** 565–78

[11] Jiang W F, Xuan SH and Gong XL 2015 The role of shear in the transition from continuous shear thickening to discontinuous shear thickening *Appl. Phys. Lett.* **106** 151902

[12] Wu X Q, Zhong F C, Yin Q Y and Huang C G 2015 Dynamic response of shear thickening fluid under laser induced shock *Appl. Phys. Lett.* **106** 071903

[13] Wyart M and Cates M E 2014 Discontinuous shear thickening without inertia in dense non-brownian suspensions *Phys. Rev. Lett.* **112** 098302

[14] Chang L, Friedrich K, Schlarb A K, Tanner R and Ye L 2011 Shear-thickening behaviour of concentrated polymer dispersions under steady and oscillatory shear *J. Mater. Sci.* **46** 339–46

[15] Maranzano B J and Wagner N J 2002 Flow-small angle neutron scattering measurements of colloidal dispersion microstructure evolution through the shear thickening transition *J. Chem. Phys.* **117** 10291–302

[16] Crawford N C, Williams S K R, Boldridge D and Liberatore M W 2013 Shear-induced structures and thickening in fumed silica slurries *Langmuir* **29** 12915–23

[17] Bender J W and Wagner N J 1995 Optical measurement of the contributions of colloidal forces to the rheology of concentrated suspensions *J. Colloid Interface Sci.* **172** 171–84

[18] Brown E and Jaeger H M 2014 Shear thickening in concentrated suspensions: phenomenology, mechanisms and relations to jamming *Rep. Prog. Phys.* **77** 046602

[19] Mari R, Seto R, Morris J F and Denn M M 2014 Shear thickening, frictionless and frictional rheologies in non-Brownian suspensions *J. Rheol.* **58** 1693–724

[20] Petford N 2009 Which effective viscosity? *Mineral Mag.* **73** 167–91

[21] Stickel J J and Powell R L 2005 Fluid mechanics and rheology of dense suspensions *Annu. Rev. Fluid. Mech.* **37** 129–49

[22] Batchelor G K 1977 The effect of Brownian motion on the bulk stress in a suspension of spherical particles *J. Fluid Mech.* **83** 97–117

[23] Doremus R H 2002 Viscosity of silica *J. Appl. Phys.* **92** 7619–29

[24] Lemke T, Bagusat F, Kohnke K, Husemann K and Mogel H J 1999 Time dependent viscosity of concentrated alumina suspensions *Colloids Surf.,* A **150** 283–7

[25] Mukherjee A, Sharma D, Chauhan S S and Singh H 2015 Time-dependent and shear-dependent transient viscosity of an alumina suspension *J. Dispersion Sci. Technol.* **36** 951–69

[26] Koke J and Modigell M 2003 Flow behaviour of semi-solid metal alloys *J. Non-Newtonian Fluid Mech.* **112** 141–60

[27] Boersma W H, Baets P J M, Laven J and Stein H N 1991 Time-dependent behavior and wall slip in concentrated shear thickening dispersions *J. Rheol.* **35** 1093–120

[28] Grizzuti N, Moldenaers P, Mortier M and Mewis J 1993 On the time-dependency of the flow-induced dynamic moduli of a liquid-crystalline hydroxypropylcellulose solution *Rheol. Acta* **32** 218–26

[29] Galindo-Rosales F J, Rubio-Hernandez F J and Sevilla A 2011 An apparent viscosity function for shear thickening fluids *J. Non-Newtonian Fluid Mech.* **166** 321–5

[30] Teng H X and Zhang J J 2013 A new thixotropic model for waxy crude *Rheol. Acta* **52** 903–11

[31] Zhang X Z, Li W H and Gong X L 2010 Thixotropy of MR shear-thickening fluids *Smart Mater. Struct.* **19** 125012

[32] Barnes H A 1997 Thixotropy—a review *J. Non-Newtonian Fluid Mech.* **70** 1–33

[33] Etemad S G and Gholamhosseini F 2002 Evaluation of time dependency of poly(ethylene glycol) solutions *Iran. Polym. J.* **11** 373–9

[34] Dullaert K and Mewis J 2005 Thixotropy: build-up and breakdown curves during flow *J. Rheol.* **49** 1213–30

[35] Dullaert K and Mewis J 2006 A structural kinetics model for thixotropy *J. Non-Newtonian Fluid Mech.* **139** 21–30

[36] Mewis J and Wagner N J 2009 *Thixotropy Adv. Colloid Interface Sci.* **147** 214–27